Entanglement and measurement-induced nonlocality of mixed maximally entangled states in multipartite dynamics

Li-Die Wang,[1] Li-Tao Wang,[1] Mou Yang,[2] Jing-Zhou Xu,[1] Z. D. Wang,[3,*] and Yan-Kui Bai[1,3,†]

[1]*College of Physics Science and Information Engineering and Hebei Advanced Thin Films Laboratory, Hebei Normal University, Shijiazhuang, Hebei 050024, China*

[2]*Laboratory of Quantum Engineering and Quantum Materials, School of Physics and Telecommunication Engineering, South China Normal University, Guangzhou 510006, China*

[3]*Department of Physics and Centre of Theoretical and Computational Physics, The University of Hong Kong, Pokfulam Road, Hong Kong, China*

(Received 19 July 2015; revised manuscript received 21 April 2016; published 7 June 2016)

The maximally entangled state can be in a mixed state as well as the well-known pure state. Taking the negativity as a measure of entanglement, we study the entanglement dynamics of bipartite, mixed maximally entangled states (MMESs) in multipartite cavity-reservoir systems. It is found that the MMES can exhibit the phenomenon of entanglement sudden death, which is quite different from the asymptotic decay of the pure-Bell-state case. We also find that maximal entanglement cannot guarantee maximal nonlocality, and the MMES does not correspond to the state with maximal measurement-induced nonlocality (MIN). In fact, the value and dynamic behavior of the MIN for the MMESs are dependent on the mixed-state probability. In addition, we investigate the distributions of negativity and the MIN in a multipartite system, where the two types of correlations have different monogamous properties.

DOI: 10.1103/PhysRevA.93.062309

I. INTRODUCTION

The maximally entangled state plays an important role in quantum information processing [1–3], including quantum teleportation [4], quantum cryptographic protocols [5], and quantum dense coding [6]. In bipartite $d \otimes d$ systems, Cavalcanti *et al.* proved that all maximally entangled states are pure states [7]. For example, in the simplest $2 \otimes 2$ systems, the pure maximally entangled state is the Bell state, which can be written as

$$|\psi\rangle = (|00\rangle + |11\rangle)/\sqrt{2} \tag{1}$$

up to local unitary transformations. Recently, it was further shown that there exist mixed maximally entangled states (MMESs) in bipartite $d \otimes d'$ systems with $d' \geqslant 2d$, which can be used as a resource for faithful teleportation [8,9]. The MMES in $2 \otimes 4$ systems has the form [8]

$$\rho = p|\psi_1\rangle\langle\psi_1| + (1-p)|\psi_2\rangle\langle\psi_2|, \tag{2}$$

where the mixed-state probability p lies in the range $(0,1)$, and the two pure-state components are $|\psi_1\rangle = (|00\rangle + |11\rangle)/\sqrt{2}$ and $|\psi_2\rangle = (|02\rangle + |13\rangle)/\sqrt{2}$.

The dynamic behavior of entanglement is a fundamental property of quantum systems. This is because unavoidable interactions with the environment may lead the entanglement of quantum systems to be degraded and, in certain cases, to disappear in a finite time (i.e., the so-called entanglement sudden death, ESD) [10–15]. López *et al.* analyzed the dynamic behavior of entangled cavity photons being affected by two dissipative reservoirs [16] and found that the entanglement of cavity photons initially in the two-qubit Bell state decays in an asymptotic manner. However, for the newly introduced MMES, its entanglement dynamic property is still an open problem, especially for a real quantum system. Since the MMES is a perfect physical resource in quantum information processing [8,9], it is desirable to investigate its dynamical property in a quantum system. This is because, once the entanglement evolution experiences the ESD, we are no longer able to concentrate the entanglement of MMES, which results in some entanglement-based quantum communication protocols losing their efficacy. In this sense, the study of the entanglement dynamic property of the MMES can provide not only useful knowledge for practical quantum operations but also the necessary information to cope with the decay of entanglement.

Nonlocality is also a kind of resource in quantum information processing [17] and has a close relationship with quantum entanglement [18]. The measurement-induced nonlocality (MIN) [19] is the maximum global effect caused by locally invariant measurement, which is different from the conventionally mentioned quantum nonlocality related to the violation of Bell's inequalities [20,21]. Moreover, the MIN can quantify the nonlocal resource in quantum communication protocols involving local measurement and a comparison between the pre- and postmeasurement states [19]. Luo and Fu proved that, for the pure Bell state, the MIN achieves the maximal value [19]. But it is not clear whether or not the MMES also has the maximal nonlocality. In particular, can the maximal entanglement guarantee the maximal nonlocality? Furthermore, in order to obtain a deep understanding of the dynamic properties of MMESs, it is helpful to analyze the entanglement and nonlocality distributions in an enlarged system including its environment.

In this paper, as quantified by entanglement negativity [22] and the MIN [19], we study the dynamic properties of the MMES in the dissipative procedure of multipartite cavity-reservoir systems. It is found that the MMES can disentangle in a finite time, which is quite different from the asymptotical

*zwang@hku.hk
†ykbai@semi.ac.cn

 ©2016 American Physical Society

decay of a pure Bell state. We also find that the MIN of the MMES is not maximal, which means that the maximal entanglement cannot guarantee the maximal nonlocality. In addition, the evolution of the MIN is dependent on the mixed probability of the MMES. Finally, we investigate the distributions of the negativity and the MIN in the multipartite system, where the squared negativity is monogamous but the MIN is not monogamous.

II. DYNAMIC PROPERTIES OF ENTANGLEMENT AND NONLOCALITY FOR THE MMES

We first recall the definition of the MMES before analyzing its dynamic properties. In $d \otimes d'$ systems, a mixed state is an MMES if and only if it has the form [8,9]

$$\rho = \sum_{m=1}^{K} p_m |\psi_m\rangle\langle\psi_m|, \tag{3}$$

where the mixed-state probabilities satisfy $\sum_{m=1}^{K} p_m = 1$ with $K \leqslant \text{floor}(d'/d)$, and the pure-state component is

$$|\psi_m\rangle = \frac{1}{\sqrt{d}} \sum_{i=0}^{d-1} |i\rangle \otimes |i + (m-1)d\rangle, \tag{4}$$

which is the maximally entangled pure state. In the following, we will study the dynamic properties of MMESs in bipartite $2 \otimes 4$ systems.

We consider a practical dynamic system of two cavities interacting with two independent reservoirs. The initial state of the four-partite system is

$$\rho_{c_1c_2r_1r_2}(0) = \rho_{c_1c_2}(0) \otimes |00\rangle\langle 00|_{r_1r_2}, \tag{5}$$

where the two reservoirs are in the vacuum state and the two cavities are in an MMES,

$$\rho_{c_1c_2}(0) = p|\psi_1\rangle\langle\psi_1| + (1-p)|\psi_2\rangle\langle\psi_2|, \tag{6}$$

with $|\psi_1\rangle = (|00\rangle + |11\rangle)/\sqrt{2}$ and $|\psi_2\rangle = (|02\rangle + |13\rangle)/\sqrt{2}$. It should be noted that, although $\rho_{c_1c_2}$ is written as a probability mix of $|\psi_1\rangle$ and $|\psi_2\rangle$, its pure-state component has the generic form $\sqrt{q}|\psi_1\rangle + e^{i\phi}\sqrt{1-q}|\psi_2\rangle$, with the parameters $q \in [0,1]$ and $\phi \in [0,2\pi]$. The interaction of a single cavity and an N-mode reservoir is described by the Hamiltonian [16,23–25]

$$\hat{H} = \hbar\omega\hat{a}^\dagger\hat{a} + \hbar\sum_{k=1}^{N} \omega_k \hat{b}_k^\dagger \hat{b}_k + \hbar\sum_{k=1}^{N} g_k(\hat{a}\hat{b}_k^\dagger + \hat{b}_k\hat{a}^\dagger). \tag{7}$$

At later times, in the limit $N \to \infty$ for the reservoirs with a flat spectrum [16], the state is given by

$$\begin{aligned}\rho_{c_1r_1c_2r_2}(t) = {} & \frac{p}{2}\left[\left(|\phi_0\rangle_{c_1r_1}|\phi_0\rangle_{c_2r_2} + \left|\phi_1^t\right\rangle_{c_1r_1}\left|\phi_1^t\right\rangle_{c_2r_2}\right)\right. \\ & \left.\times\left(\langle\phi_0|_{c_1r_1}\langle\phi_0|_{c_2r_2} + \left\langle\phi_1^t\right|_{c_1r_1}\left\langle\phi_1^t\right|_{c_2r_2}\right)\right] \\ & + \frac{1-p}{2}\left[\left(|\phi_0\rangle_{c_1r_1}\left|\phi_2^t\right\rangle_{c_2r_2} + \left|\phi_1^t\right\rangle_{c_1r_1}\left|\phi_3^t\right\rangle_{c_2r_2}\right)\right. \\ & \left.\times\left(\langle\phi_0|_{c_1r_1}\left\langle\phi_2^t\right|_{c_2r_2} + \left\langle\phi_1^t\right|_{c_1r_1}\left\langle\phi_3^t\right|_{c_2r_2}\right)\right],\end{aligned} \tag{8}$$

where the components can be written as

$$\begin{aligned}|\phi_0\rangle &= |00\rangle, \\ \left|\phi_1^t\right\rangle &= \xi|10\rangle + \chi|01\rangle, \\ \left|\phi_2^t\right\rangle &= \xi^2|20\rangle + \sqrt{2}\xi\chi|11\rangle + \chi^2|02\rangle, \\ \left|\phi_3^t\right\rangle &= \xi^3|30\rangle + \sqrt{3}\xi^2\chi|21\rangle + \sqrt{3}\xi\chi^2|12\rangle + \chi^3|03\rangle,\end{aligned} \tag{9}$$

in which the amplitudes are $\xi(t) = e^{-\kappa t/2}$ and $\chi(t) = (1 - e^{-\kappa t})^{1/2}$, with the parameter κ being the dissipative constant [26].

In this section, we focus on the dynamic properties of two cavities which are initially in an MMES. As the cavities and reservoirs interact, the state of two cavities is $\rho_{c_1c_2}(t) = \text{Tr}_{r_1r_2}[\rho_{c_1r_1c_2r_2}(t)]$, which has the matrix form

$$\rho_{c_1c_2}(t) = \begin{pmatrix} a_{11} & 0 & 0 & 0 & 0 & a_{16} & 0 & 0 \\ 0 & a_{22} & 0 & 0 & 0 & 0 & a_{27} & 0 \\ 0 & 0 & a_{33} & 0 & 0 & 0 & 0 & a_{38} \\ 0 & 0 & 0 & a_{44} & 0 & 0 & 0 & 0 \\ 0 & 0 & 0 & 0 & a_{55} & 0 & 0 & 0 \\ a_{61} & 0 & 0 & 0 & 0 & a_{66} & 0 & 0 \\ 0 & a_{72} & 0 & 0 & 0 & 0 & a_{77} & 0 \\ 0 & 0 & a_{83} & 0 & 0 & 0 & 0 & a_{88} \end{pmatrix} \tag{10}$$

with the basis in the order $\{|00\rangle, |01\rangle, |02\rangle, |03\rangle, |10\rangle, |11\rangle, |12\rangle, |13\rangle\}$ and the matrix elements

$$\begin{aligned} a_{11} &= (p + \chi^4 + \chi^8 - p\chi^8)/2, \\ a_{22} &= \xi^2\chi^2[2 - p + 3(1-p)\chi^4]/2, \\ a_{33} &= (1-p)\xi^4(1 + 3\chi^4)/2, \\ a_{44} &= (1-p)\xi^6\chi^2/2, \\ a_{55} &= \xi^2\chi^2(p + \chi^4 - p\chi^4)/2, \\ a_{66} &= \xi^4[p + 3(1-p)\chi^4]/2, \\ a_{77} &= 3(1-p)\xi^6\chi^2/2, \\ a_{88} &= (1-p)\xi^8/2, \\ a_{16} &= a_{61} = \xi^2[p + \sqrt{3}(1-p)\chi^4]/2, \\ a_{27} &= a_{72} = \sqrt{3/2}(1-p)\xi^4\chi^2, \\ a_{38} &= a_{83} = (1-p)\xi^6/2. \end{aligned} \tag{11}$$

In order to characterize the dynamic entanglement properties of two cavities, we need to choose a suitable measure of entanglement. Here, we use the negativity [22] to quantify the entanglement of two cavities due to its computability for any state of an arbitrary bipartite system. For the quantum state $\rho_{c_1c_2}(t)$, its negativity is

$$N_{c_1c_2}(t) = \frac{\left|\left|\rho_{c_1c_2}^{T_{c_1}}(t)\right|\right| - 1}{2} = \frac{\sum_{i=1}^{8}|\lambda_i| - 1}{2}, \tag{12}$$

where $||\cdot||$ is the trace norm and equal to the sum of the moduli of the eigenvalues for the Hermitian matrix $\rho_{c_1c_2}^{T_{c_1}}(t)$, which is the partial transpose with respect to the subsystem c_1

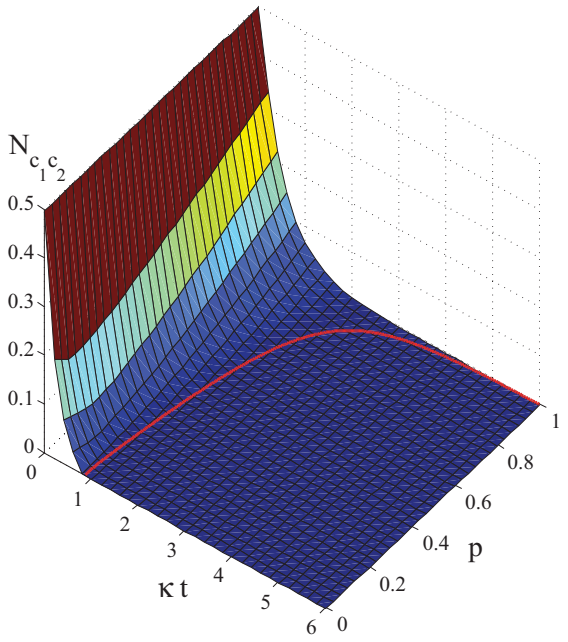

FIG. 1. Evolution of entanglement of the MMES in two cavities, where the negativity is shown as a function of the time κt and the probability p. The red line indicates the entanglement sudden death of the two cavities.

[22]. After some derivation, we can obtain the eigenvalues

$$\begin{aligned}
\lambda_1 &= (1-p)\xi^8/2,\\
\lambda_2 &= (p+\chi^4+\chi^8-p\chi^8)/2,\\
\lambda_3 &= \xi^4\{[1+(6-6p)\chi^4]-\sqrt{A}\}/4,\\
\lambda_4 &= \xi^4\{[1+(6-6p)\chi^4]+\sqrt{A}\}/4,\\
\lambda_5 &= [2(1-p)\xi^6\chi^2-\sqrt{B}]/2,\\
\lambda_6 &= [2(1-p)\xi^6\chi^2+\sqrt{B}]/2,\\
\lambda_7 &= \xi^2\{\chi^2[1+2(1-p)\chi^4]-\sqrt{C}\}/2,\\
\lambda_8 &= \xi^2\{\chi^2[1+2(1-p)\chi^4]+\sqrt{C}\}/2, \qquad (13)
\end{aligned}$$

where the parameters are $A=(1-2p)^2+24(1-p)^2\chi^4$, $B=(1-p)\xi^{12}(1+\chi^4)$, and $C=p^2+(1-p)[1+(2\sqrt{3}-1)p]\chi^4+5(1-p)^2\chi^8+(1-p)^2\chi^{12}$.

In Fig. 1, we plot the negativity $N_{c_1c_2}(t)$ as a function of the time κt and the probability p. As seen from Fig. 1, when $\kappa t = 0$, the quantum state $\rho_{c_1c_2}$ is the MMES, and its negativity has the maximal value of 0.5 regardless of the choice of probability p. For a given value of the probability, p, the negativity decreases as the time κt increases. It should be pointed out that as time increases, the entanglement of the MMES decays through sudden death rather than asymptotically like the two-qubit Bell state. The red line in Fig. 1 indicates the time of the ESD for the negativity $N_{c_1c_2}(t)$ and satisfies the equation

$$p=\frac{1-\sqrt{3}+3\chi^4-3\chi^8+\sqrt{D}}{1-2\sqrt{3}+\chi^{-4}+5\chi^4-3\chi^8}, \qquad (14)$$

where the parameter $D=3-2\sqrt{3}+4(2-\sqrt{3})\chi^4+\chi^8$, with $\chi=\sqrt{1-e^{-\kappa t}}$ (the derivation of the ESD line is presented in Appendix A). When the probability $p=0$, the initial state of the two cavities is $|\psi_2\rangle=(|02\rangle+|13\rangle)/\sqrt{2}$, which is a two-qubit pure maximal entangled state with qubit c_1 involving states 0 and 1 and qubit c_2 involving states 2 and 3. As the system evolves, the quantum state of two cavities becomes a $2\otimes 4$ system and has the matrix form shown in Eq. (10) with the parameter $p=0$. Its entanglement evolution shows the ESD phenomenon, and the negativity becomes zero at the time $\kappa t=\ln[(3+\sqrt{3})/2]\approx 0.8612$. When the probability $p\in(0,1)$, the initial state $\rho_{c_1c_2}(0)$ is the MMES. The ESD time of the two cavities is determined by Eq. (14) and increases as a function of the probability p. In the $p=1$ case, the initial state is the two-qubit Bell state $|\psi_1\rangle=(|00\rangle+|11\rangle)/\sqrt{2}$, and its entanglement disappears at the time $\kappa t\to\infty$, which coincides with the result for asymptotic decay presented by López *et al.* [16].

Here, we have shown that, unlike the asymptotic entanglement decay of the Bell state, the MMES of two cavities experiences the ESD in the dissipative procedure of cavity-reservoir systems. It is argued that the high-dimensional component $|\psi_2\rangle=|02\rangle+|13\rangle)/\sqrt{2}$ plays the dominant role. Although the initial state $|\psi_2\rangle$ is a logic two-qubit state, it will evolve to a $2\otimes 4$ system along with the cavity-reservoir interaction, which results in the ESD phenomenon of two cavities. In the evolution of two cavities, the ESD time is postponed when the mixed probability of the component $|\psi_1\rangle$ (the Bell state) increases. In the case of $p=1$ for the MMES, the component $|\psi_2\rangle$ disappears, and there is no ESD phenomenon, which is just the evolution of the pure Bell state $|\psi_1\rangle=(|00\rangle+|11\rangle)/\sqrt{2}$.

In addition to quantum entanglement, nonlocality is also a useful resource in quantum secure communication. It is worthwhile to further investigate whether maximally entangled states like the MMES also result in maximal nonlocality and how the nonlocality of the MMES evolves with time. The MIN [19] is a computable nonlocality measure, which is the maximum global effect caused by locally invariant measurement. The MIN is defined as [19]

$$\mathrm{MIN}(\rho_{AB})=\max_{\Pi^A}||\rho-\Pi^A(\rho_{AB})||^2, \qquad (15)$$

where the max runs over all the von Neumann measurements $\Pi^A=\{\Pi_k^A\}$ which do not disturb the reduced density matrix ρ_A (i.e., $\sum_k \Pi_k^A\rho_A\Pi_k^A=\rho_A$), and the Hilbert-Schmidt norm is $||X||^2=\mathrm{tr}X^\dagger X$. The state of the two cavities $\rho_{c_1c_2}(t)$ in Eq. (10) can be rewritten in a generalized Bloch form,

$$\begin{aligned}
\rho_{c_1c_2}(t)=\frac{1}{2\sqrt{2}}\frac{I_2}{\sqrt{2}}\otimes\frac{I_4}{2}+\sum_{i=1}^{3}x_iX_i\otimes\frac{I_4}{2}+\frac{I_2}{\sqrt{2}}\\
\otimes\sum_{j=1}^{15}y_jY_j+\sum_{i=1}^{3}\sum_{j=1}^{15}T_{ij}X_i\otimes Y_j, \qquad (16)
\end{aligned}$$

where I_2 and I_4 are identity matrices of the subsystems and $X_i=\sigma_i/\sqrt{2}$ and $Y_j=(\sigma_{j'}\otimes\sigma_{j''})/2$ are operator bases with $j',j''\in\{0,1,2,3\}$ except for the case $j'=j''=0$ (here, $\sigma_0=I_2$ and $\{\sigma_1,\sigma_2,\sigma_3\}$ are the Pauli matrices). In the Bloch

expression, Eq. (16), the matrix elements are

$$\begin{aligned} x_i &= \mathrm{tr}\big(\rho_{c_1c_2} X_i \otimes I_4/2\big), \\ y_j &= \mathrm{tr}\big(\rho_{c_1c_2} I_2/\sqrt{2} \otimes Y_j\big), \\ T_{ij} &= \mathrm{tr}\big(\rho_{c_1c_2} X_i \otimes Y_j\big). \end{aligned} \tag{17}$$

Luo and Fu derived an analytical formula for the MIN in an arbitrary $2 \otimes d$ system [19],

$$\mathrm{MIN}_{c_1c_2} = \begin{cases} \mathrm{tr}TT^t - \frac{1}{\|\mathbf{x}\|^2}\mathbf{x}^t TT^t\mathbf{x} & \text{if} \quad \mathbf{x} \neq 0, \\ \mathrm{tr}TT^t - \lambda_3 & \text{if} \quad \mathbf{x}=0, \end{cases} \tag{18}$$

where λ_3 is the minimum eigenvalue of the 3×3 matrix TT^t with $T = (T_{ij})$ and $\mathbf{x} = (x_1, x_2, x_3)^t$ is the local Bloch vector with the norm $||\mathbf{x}||^2 = \sum_i x_i^2$ (here, t represents the transposition). After some derivation, we can obtain the expression for the MIN of two dissipative cavities, which can be written as

$$\mathrm{MIN}_{c_1c_2}(t) = \tfrac{1}{2}\xi^4[F - 2p(F-G) + p^2(1-2G+F)], \tag{19}$$

where the two parameters are $F = \xi^8 + 6\xi^4\chi^4 + 3\chi^8$ and $G = \sqrt{3}\chi^4$, with $\xi = e^{-\kappa t/2}$ and $\chi = \sqrt{1-e^{-\kappa t}}$. The details of the calculation and the continuity analysis of the MIN are presented in Appendix B.

In Fig. 2, we plot the MIN as a function of the time κt and the probability p. When $\kappa t = 0$, $\rho_{c_1c_2}(0)$ is the MMES, and its nonlocality is

$$\mathrm{MIN}_{c_1c_2}(0) = \big(p - \tfrac{1}{2}\big)^2 + \tfrac{1}{4}, \tag{20}$$

which is symmetric to the probability $p = 1/2$. As shown in Fig. 2, the MIN has the maximum value of 0.5 for the cases of $p = 0$ and $p = 1$, which correspond to the pure maximally entangled states $|\psi_2\rangle$ and $|\psi_1\rangle$. When $p \in (0,1)$, the MIN has less than the maximum value and reaches the minimum value of 0.25 at $p = 0.5$. Therefore, we can reach the conclusion that the nonlocality of the MMES is not maximal, although its entanglement is maximal for any value of the probability p. According to Eq. (20), we find that the MIN is directly proportional to the purity $\mathrm{Tr}(\rho^2)$ of the MMES, i.e., $\mathrm{MIN}_{c_1c_2}(0) = \frac{1}{2}\mathrm{Tr}[\rho^2_{c_1c_2}(0)]$. When the mixed-state probability of the MMES changes from 0 to 1/2, its purity decreases, which results in the MIN changing from the maximum of 0.5 to the minimum of 0.25. When the probability p changes from 1/2 to 1, the purity of the MMES also increases, and the MIN changes from the minimum of 0.25 to the maximum of 0.5. As two cavities evolve, $\mathrm{MIN}_{c_1c_2}(t)$ decays in an asymptotic manner and disappears in the limit $\kappa t \to \infty$. This is different from the sudden-death evolution of the negativity of two cavities since the nonlocality described by the MIN contains both quantum and classical correlations. The inset of Fig. 2 shows the difference $\mathrm{MIN}_{p=1} - \mathrm{MIN}_{p=0}$, which indicates that the nonlocality is no longer symmetric as the system evolves.

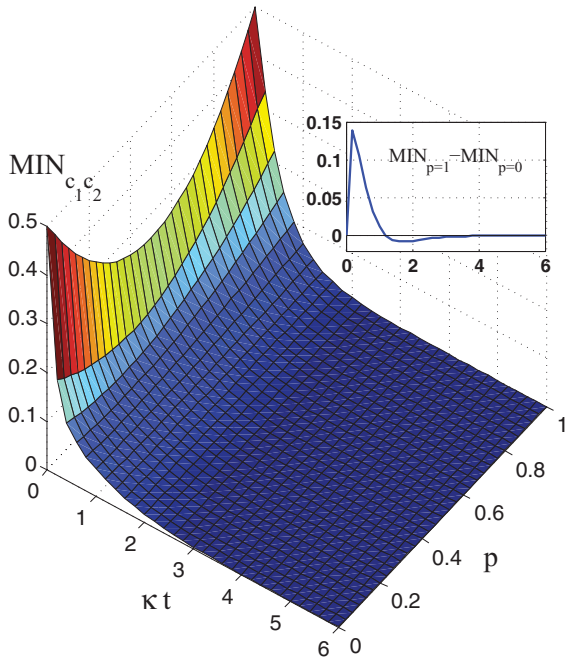

FIG. 2. Evolution of the MIN of the MMES in two cavities, where the nonlocality is shown as a function of the time κt and the probability p. The inset is the difference $\mathrm{MIN}_{p=1} - \mathrm{MIN}_{p=0}$ as a function of κt.

III. ENTANGLEMENT AND NONLOCALITY DISTRIBUTIONS OF THE MMES IN MULTIPARTITE DYNAMICS

Entanglement monogamy is an important property of multipartite systems and means that quantum entanglement cannot be freely shared among many parties [27–32]. It has been proved that the squared negativity obeys the monogamy inequality in pure states of qubit systems, $N^2_{A_1|A_2\cdots A_n} - N^2_{A_1A_2} - \cdots - N^2_{A_1A_n} \geqslant 0$ [33]. However, for mixed states or multilevel pure-state systems, whether or not a similar monogamy relation holds is still an open problem. Recently, a numerical analysis was carried out for tripartite multilevel pure states [34], which supported the monogamy relations for squared negativity. However, it is still unknown whether or not the monogamous relation holds for the four-partite case, especially in a real quantum system with dissipative reservoirs. With this in mind, we next analyze the negativity distribution of the MMES in the four-partite $2 \otimes 2 \otimes 4 \otimes 4$ cavity-reservoir systems. On the one hand, this analysis can verify the monogamy inequality for the squared negativity, and on the other hand, it can provide a deep understanding of the dynamics of the MMES.

The residual entanglement in monogamy inequalities can be used as a multipartite entanglement measure or indicator to characterize the structure of multipartite entanglement [35–39]. For composite cavity-reservoir systems, we analyze the entanglement distribution in the partition $c_1r_1|c_2r_2$ and evaluate the multipartite entanglement indicator

$$\begin{aligned} M_{c_1r_1|c_2r_2}(t) = N^2_{c_1r_1|c_2r_2}(t) - N^2_{c_1c_2}(t) - N^2_{c_1r_2}(t) \\ - N^2_{r_1c_2}(t) - N^2_{r_1r_2}(t). \end{aligned} \tag{21}$$

As the system evolves, the four-partite negativity is invariant and satisfies the relation $N_{c_1r_1|c_2r_2}(t) = N_{c_1r_1|c_2r_2}(0) = N_{c_1c_2}(0) = 0.5$ since the local dissipation is unitary and the two reservoirs are in the vacuum state initially. At a later time, the state of the two reservoirs has a form similar to that of the two cavities, and we get the relation $\rho_{r_1r_2}(t) = S_{\xi\leftrightarrow\chi}[\rho_{c_1c_2}(t)]$ in

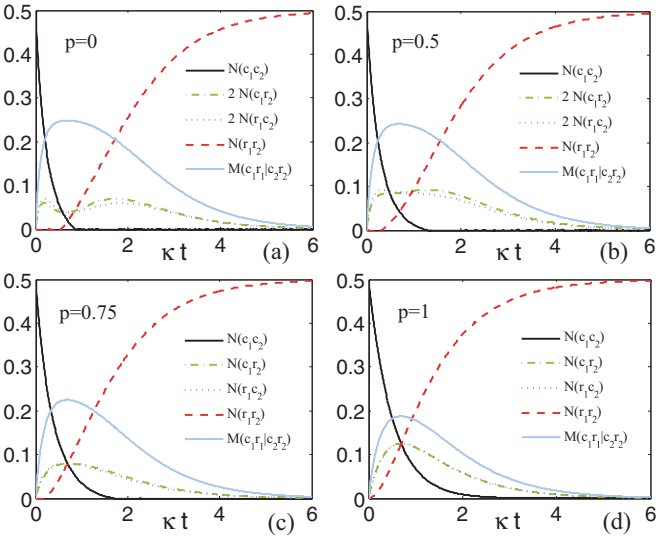

FIG. 3. The distribution of negativity in the dissipation of multipartite $2 \otimes 2 \otimes 4 \otimes 4$ cavity-reservoir systems, where the non-negative values of $M_{c_1r_1|c_2r_2}$ indicate multipartite entanglement.

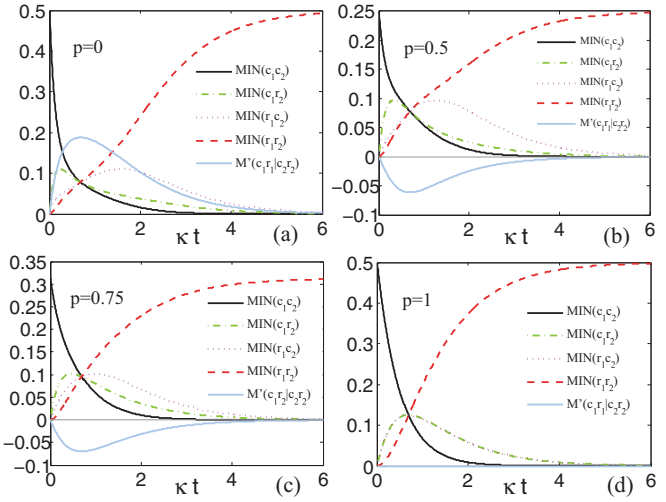

FIG. 4. The MIN distribution of the MMES in multipartite $2 \otimes 2 \otimes 4 \otimes 4$ cavity-reservoir systems, where the residual nonlocality $M'_{c_1r_1|c_2r_2}$ can be positive, zero, or negative as a function of the time parameter κt.

which $S_{\xi\leftrightarrow\chi}$ is an operation exchanging two parameters (i.e., $\xi \to \chi$ and $\chi \to \xi$). Thus, the negativity of the reservoirs is

$$N_{r_1r_2}(t) = S_{\xi\leftrightarrow\chi}\big[N_{c_1c_2}(t)\big]. \tag{22}$$

We can also derive the relationship $\rho_{r_1c_2}(t) = S_{\xi\leftrightarrow\chi}[\rho_{c_1r_2}(t)]$ and the negativities

$$N_{r_1c_2}(t) = S_{\xi\leftrightarrow\chi}\big[N_{c_1r_2}(t)\big] \tag{23}$$

for subsystems c_1r_2 and r_1c_2. A more detailed description of the density matrix $\rho_{c_1r_2}(t)$ and its negativity $N_{c_1r_2}(t)$ can be found in Appendix C.

In Fig. 3, we plot the negativity distribution as a function of the time κt for the cases where the probability p of the MMES is chosen to be 0,0.5,0.75, and 1. As time increases, the two reservoirs exhibit the phenomenon of entanglement sudden birth (ESB) [16], which corresponds to the ESD of the two cavities. As the probability p increases, the ESB time is advanced, and the ESD time is delayed, as shown in Figs. 3(a)–3(c). When the probability is $p = 1$, both the ESB and ESD phenomena disappear, as shown in Fig. 3(d), since the initial state becomes the two-qubit Bell state. For the subsystems c_1r_2 and r_1c_2, the negativities have two peak values when the probability is $p = 0$ and $p = 0.5$ [see Figs. 3(a) and 3(b), where we multiply $N_{c_1r_2}$ and $N_{r_1c_2}$ by a factor of 2 for clarity]. As the probability p increases, the number of peaks in the negativity changes from two to one, as shown in Figs. 3(c) and 3(d). We further calculated the entanglement distribution in Eq. (21) and found that the squared negativity is monogamous in the composite cavity-reservoir systems. Therefore, the quantity $M_{c_1r_1|c_2r_2}(t)$ can serve as a multipartite entanglement indicator as time evolves, as plotted (solid blue line) in Fig. 3 for different probabilities.

Next, we analyze the MIN distribution of the MMES in the multipartite cavity-reservoir system. It has been proved that the MIN is not monogamous in multiqubit systems [40,41]. However, whether the MIN is monogamous in multipartite multilevel systems needs to be further investigated, especially for the newly introduced MMES. Using the relationships of the density matrices $\rho_{c_1c_2}$, $\rho_{c_1r_2}$, $\rho_{r_1c_2}$, and $\rho_{r_1r_2}$, we can get

$$\begin{aligned} \mathrm{MIN}_{r_1r_2}(t) &= S_{\xi\leftrightarrow\chi}\big[\mathrm{MIN}_{c_1c_2}(t)\big], \\ \mathrm{MIN}_{r_1c_2}(t) &= S_{\xi\leftrightarrow\chi}\big[\mathrm{MIN}_{c_1r_2}(t)\big], \end{aligned} \tag{24}$$

where $S_{\xi\leftrightarrow\chi}$ is the exchanging operation acting on the parameters ξ and χ. After a derivation similar to that for $\mathrm{MIN}_{c_1c_2}(t)$, we can obtain the MIN of the subsystem c_1r_2,

$$\mathrm{MIN}_{c_1r_2}(t) = \tfrac{1}{2}\xi^2\chi^2[p^2 + 2\sqrt{3}p(1-p)\xi^4 + F_1], \tag{25}$$

with the parameter $F_1 = (3\xi^8 + 6\xi^4\chi^4 + \chi^8)(1-p)^2$. In addition, for the MIN of multipartite cavity-reservoir systems in the partition $c_1r_1|c_2r_2$, we can obtain the expression

$$\mathrm{MIN}_{c_1r_1|c_2r_2}(t) = \mathrm{MIN}_{c_1r_1|c_2r_2}(0) = \tfrac{1}{2}(1 - 2p + 2p^2), \tag{26}$$

where the MIN is invariant as the time increases because the evolution operation $U_{c_1r_1}(\hat{H},t) \otimes U_{c_2r_2}(\hat{H},t)$ is locally unitary. In addition, we calculate the MIN distribution $M'_{c_1r_1|c_2r_2}(t) = \mathrm{MIN}_{c_1r_1|c_2r_2}(t) - \mathrm{MIN}_{c_1c_2}(t) - \mathrm{MIN}_{c_1r_2}(t) - \mathrm{MIN}_{r_1c_2}(t) - \mathrm{MIN}_{r_1r_2}(t)$, which is written as

$$M'_{c_1r_1|c_2r_2}(t) = (1-p)\xi^2\chi^2(G_1 - \sqrt{3}p), \tag{27}$$

with the parameter $G_1 = (1-p)(1-\chi^2+\chi^4)$.

In Fig. 4, we plot the distribution of the MIN as a function of time κt with different probabilities p for the MMES. As time increases, the MIN of two cavities decreases asymptotically, and the MIN of the two reservoirs increases asymptotically. When the time $\kappa t \to \infty$, the MIN of the two cavities transfers completely to the reservoirs. For the subsystems c_1r_2 and r_1c_2, the MINs first increase to their maximums and then decay asymptotically. As the probability increases, the distance between the two peaks of $\mathrm{MIN}_{c_1r_2}$ and $\mathrm{MIN}_{r_1c_2}$ becomes smaller. When the probability is $p = 1$, the distance goes to zero, and the two MINs coincide completely, as shown in Fig. 4(d). Unlike the distribution of entanglement negativity, the MIN in the multipartite systems is not always

monogamous. When the mixed-state probability is $p = 0$, the MIN is monogamous, and the indicator $M'_{c_1r_1|c_2r_2}(t)$ (the solid blue line) is nonnegative, as shown in Fig. 4(a). However, when the probabilities are $p = 0.5$ and $p = 0.75$, the MINs are polygamous, and $M'_{c_1r_1|c_2r_2}(t)$ is no longer positive [see Figs. 4(b) and 4(c)]. When the probability is $p = 1$, the MMES becomes the two-qubit Bell state, and the indicator $M'_{c_1r_1|c_2r_2}(t)$ is zero at all times for cavity-reservoir systems, as shown in Fig. 4(d). The different distribution property from that of entanglement negativity indicates that the MIN and entanglement are two inequivalent types of resources for quantum information processing.

Although the MIN itself is not monogamous in multipartite multilevel systems, its functions may possess this property. For example, the quantum discord [42,43] is not monogamous even in three-qubit pure states [44–47], but the squared quantum discord is monogamous in an arbitrary three-qubit pure state [48,49]. Recently, similar situations for the entanglement of formation have also been discussed [31,50–54]. For the MIN in multipartite cavity-reservoir systems, we calculated the square of the MIN, and the numerical result supports the monogamy relation. However, in the general case, an analytical proof for the monogamy property of the squared MIN is still an open problem.

IV. DISCUSSION AND CONCLUSION

We have studied the dynamic behavior of the MMES over the course of the dissipative evolution of multipartite multilevel cavity-reservoir systems. It has been found that, unlike the two-qubit Bell state $|\psi_1\rangle = (|00\rangle + |11\rangle)/\sqrt{2}$, whose negativity decays in an asymptotic manner [16], the entanglement dynamics of the MMES exhibits the ESD phenomenon, as shown in Fig. 1. Therefore, as an entanglement resource, the MMES is not superior to the pure two-qubit Bell state in this dissipative system. We think that the high-dimensional component $|\psi_2\rangle = (|02\rangle + |13\rangle)/\sqrt{2}$ in the MMES gives rise to the ESD of the two cavities' evolution. Moreover, we further study the MMESs in $2 \otimes 6$ and $2 \otimes 8$ systems where the component $|\psi_2\rangle$ is replaced by the higher-dimensional components $|\psi_3\rangle = (|04\rangle + |15\rangle)/\sqrt{2}$ and $|\psi_4\rangle = (|06\rangle + |17\rangle)/\sqrt{2}$, respectively. The analytical results show that the new MMESs still experience the ESD in the dynamical evolution (the details for the calculation are given in Appendix D), which further supports our viewpoint.

The MIN has a close relation with quantum communication protocols involving local measurement and a comparison between the pre- and postmeasurement states [19]. We find that maximal entanglement *cannot* guarantee maximal nonlocality. As shown in Fig. 2, the MIN of the MMES is not maximal, and its value is directly proportional to the purity $\mathrm{Tr}(\rho^2)$ of the MMES, which is quite different from the situation of the Bell state exhibiting maximal nonlocality. For the MMESs with higher-dimensional components, their MINs are also dependent on the mixed-state probability p, and the nonlocality evolutions are asymptotical (the details are given in Appendix E). We explain that the decrease of the MIN of the MMESs is due to the decrease of their purity, and the MIN evolution of the MMESs is asymptotic since this kind of nonlocality contains both quantum and classical correlations [19]. For the quantum nonlocality related to the violation of Bell inequalities [55–60], its relation to the maximal entangled state is still an open problem yet to be addressed.

In order to obtain a deep understanding of the dynamic properties of the MMES, we have investigated its entanglement and nonlocality distributions in multipartite systems. The numerical results have shown that the squared negativity is monogamous in multipartite cavity-reservoir systems (beyond the four values of probability p shown in Fig. 3, we further calculated the distribution for p ranging across $[0,1]$). Moreover, for the MMESs of $2 \otimes 6$ and $2 \otimes 8$ systems, our numerical calculation still shows that the squared negativity is monogamous in the multipartite dissipative systems. These results support the conjecture of He and Vidal [34] that the squared negativity is monogamous in multipartite multilevel systems. On the other hand, the MIN distribution of the MMES is not monogamous in the multipartite cavity-reservoir system, as shown in Fig. 4, which indicates that the MIN is a different type of resource from entanglement in quantum information processing. We further investigate the MIN distributions for the MMESs with higher-dimensional components and find that the MIN is still not monogamous (the details are shown in Appendix E).

In conclusion, we have studied the dynamic behavior of the MMES in multipartite cavity-reservoir systems. It has been found that the evolution of the negativity of the MMES exhibits the ESD phenomenon and is not superior to the two-qubit Bell state as an entanglement resource in a dissipative system. We also found that maximal entanglement cannot guarantee maximal nonlocality. The MIN of the MMES is not maximal, and its evolution is dependent on the mixed-state probability of the MMES. In addition, we have investigated the distributions of the negativity and the MIN of the MMESs in the multipartite cavity-reservoir systems, where two types of correlation exhibit different monogamous properties.

ACKNOWLEDGMENTS

Y.-K.B. is grateful to Prof. N. Davison for critical reading of the manuscript and also would like to thank Y.-F. Xu for many useful discussions. This work was supported by the URC fund of HKU, NSF-China under Grants No. 11575051 and No. 11274124, Hebei NSF under Grant No. A2016205215, and the funds of Hebei Normal University under Grants No. L2008B03 and No. L2012B06.

APPENDIX A: THE DERIVATION OF THE ESD LINE FOR NEGATIVITY $N_{c_1c_2}$

In Eq. (12) of the main text, the negativity $N_{c_1c_2}(t)$ is determined via the sum of absolute values of the negative eigenvalues. After some analysis, we find that the eigenvalues $\{\lambda_1,\lambda_2,\lambda_4,\lambda_6,\lambda_8\}$ are always nonnegative, while the other eigenvalues $\{\lambda_3,\lambda_5,\lambda_7\}$ can be positive, zero, or negative. Therefore, as the two cavities evolve, the negativity $N_{c_1c_2}(t)$ becomes zero when the three eigenvalues $\{\lambda_3,\lambda_5,\lambda_7\}$ become nonnegative.

Using the expressions for λ_3, λ_5, and λ_7 in Eq. (13), we can derive the $p \sim \kappa t$ relations when these eigenvalues are zero.

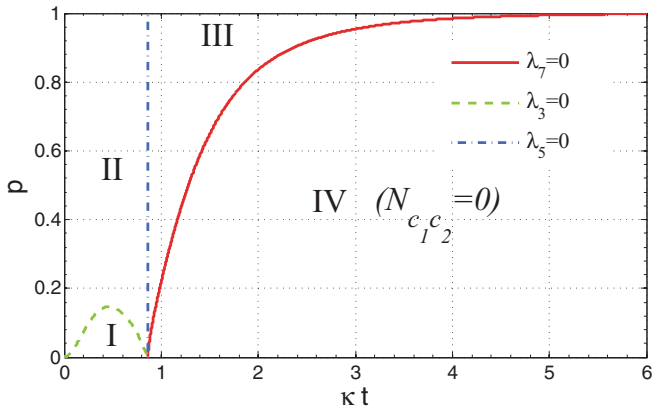

FIG. 5. Four regions in the entanglement evolution of two cavities, where, in region IV, all three eigenvalues $(\lambda_3,\lambda_5,\lambda_7)$ are positive and the negativity $N_{c_1c_2}$ becomes zero.

When $\lambda_3 = 0$, we have the relation

$$p = \frac{3(e^{\kappa t}-1)^2(3-6e^{\kappa t}+2e^{2\kappa t})}{9-36e^{\kappa t}+48e^{2\kappa t}-24e^{3\kappa t}+2e^{4\kappa t}}. \tag{A1}$$

For the case $\lambda_5 = 0$, we have

$$\kappa t = \ln[(3+\sqrt{3})/2] \tag{A2}$$

for an arbitrary value of parameter p. When $\lambda_7 = 0$, we can derive the $p \sim \kappa t$ relation as shown in Eq. (14) of the main text. In Fig. 5, we plot the three relations in the plane of parameters p and κt, where the dashed green line is for $\lambda_3 = 0$, the dot-dashed blue line is for $\lambda_5 = 0$, and the solid red line is for $\lambda_7 = 0$. The three lines divide the whole area into four parts. In regions I, II, and III, the signs of the eigenvalues $(\lambda_3,\lambda_5,\lambda_7)$ are $(-,-,-)$, $(+,-,-)$, and $(+,+,-)$, which result in nonzero negativity for the two cavities. In region IV, all the eigenvalues are positive, leading to the negativity being $N_{c_1c_2}(t) = 0$. Thus, as seen from Fig. 5, the red line for $\lambda_7 = 0$ determines the ESD time of the two cavities, which is described by Eq. (14) of the main text.

APPENDIX B: CALCULATION AND CONTINUITY ANALYSIS FOR THE MIN OF TWO CAVITIES

Before evaluating the nonlocality $\mathrm{MIN}_{c_1c_2}(t)$ given in Eq. (18), we first calculate the local Bloch vector $\mathbf{x}$ and correlation matrix T. According to Eq. (17), the local Bloch vector of subsystem c_1 is

$$\mathbf{x} = \left(0,0,\frac{\chi^2}{2\sqrt{2}}\right)^t, \tag{B1}$$

which leads to the norm being $||\mathbf{x}||^2 = \chi^4/8$, with $\chi = \sqrt{1-e^{-\kappa t}}$. The correlation matrix $T = T'/2\sqrt{2}$ is a 3×15 matrix, in which the nonzero elements of T' are

$$\begin{aligned}
T'_{1,1} &= -T_{2,2} = \xi^2[p+(1-p)\xi^4+\sqrt{3}(1-p)\chi^4],\\
T'_{3,3} &= (1-2\chi^2+2\chi^4)[1-4(1-p)\xi^2\chi^2],\\
T'_{1,5} &= T'_{1,10} = T'_{2,6} = -T'_{2,9} = \sqrt{6}(1-p)\xi^4\chi^2,\\
T'_{1,13} &= \xi^2[p-(1-p)\xi^4+\sqrt{3}(1-p)\chi^4],\\
T'_{2,14} &= -\xi^2[p-(1-p)\xi^4+\sqrt{3}(1-p)\chi^4],\\
T'_{3,12} &= \chi^2-4(1-p)\xi^4\chi^4,\\
T'_{3,15} &= 2p-1+(4-6p)\chi^2-(8-10p)\chi^4+6(1-p)\chi^6,
\end{aligned} \tag{B2}$$

with $\xi = e^{-\kappa t/2}$. When $\kappa t > 0$, we have the local Bloch vector $\mathbf{x} \neq 0$. After substituting the three terms $\mathbf{x}$, $||\mathbf{x}||^2$, and T into the first formula in Eq. (18), we can obtain the expression for $\mathrm{MIN}_{c_1c_2}(t>0)$ in Eq. (19). When $\kappa t = 0$, the quantum state $\rho_{c_1c_2}(0)$ is the MMES for which the local Bloch vector is $\mathbf{x} = 0$. In this case, we need to calculate the eigenvalues of matrix TT^t, which are $\lambda_1 = \lambda_2 = \lambda_3 = (1-2p+2p^2)/4$. According to the second formula in Eq. (18), we can derive $\mathrm{MIN}_{c_1c_2}(0) = (1-2p+2p^2)/2$.

Next, we prove the continuity of $\mathrm{MIN}_{c_1c_2}(t)$. Based on the previous analysis, we know that the two formulas in Eq. (18) are used for the cases $\mathbf{x} \neq 0$ and $\mathbf{x} = 0$, which correspond to the time evolutions $\kappa t > 0$ and $\kappa t = 0$, respectively. If $\mathrm{MIN}_{c_1c_2}$ is continuous, the limit of $\mathrm{MIN}_{c_1c_2}(\kappa t \to 0_+)$ in the first formula should coincide with the value of $\mathrm{MIN}_{c_1c_2}(\kappa t = 0)$. After some calculation, we can get

$$\begin{aligned}
\lim_{\kappa t\to 0_+}\frac{\mathbf{x}^t TT^t\mathbf{x}}{\|\mathbf{x}\|^2} &= \lim_{\kappa t\to 0_+}\frac{\frac{d(\mathbf{x}^t TT^t\mathbf{x})}{d(\kappa t)}}{\frac{d(\|\mathbf{x}\|^2)}{d(\kappa t)}} = \lim_{\kappa t\to 0_+}\frac{\frac{d^2(\mathbf{x}^t TT^t\mathbf{x})}{d(\kappa t)^2}}{\frac{d^2(\|\mathbf{x}\|^2)}{d(\kappa t)^2}}\\
&= \frac{\frac{1}{16}(1-2p+2p^2)}{\frac{1}{4}} = \lambda_3,
\end{aligned} \tag{B3}$$

where we have used L'Hôpital's rule and λ_3 is the minimal eigenvalue of matrix TT^t. Then, in the limit $\kappa t \to 0_+$, the two formulas in Eq. (18) are continuous, and we have

$$\lim_{\kappa t\to 0_+}\mathrm{MIN}_{c_1c_2}(\kappa t) = \mathrm{MIN}_{c_1c_2}(0) = \tfrac{1}{2}(1-2p+2p^2). \tag{B4}$$

As a result, the nonlocality $\mathrm{MIN}_{c_1c_2}(t)$ can be described by Eq. (19) of the main text throughout the entire period of the dynamic evolution.

APPENDIX C: THE DENSITY MATRIX $\rho_{c_1r_2}$ AND ITS NEGATIVITY $N_{c_1r_2}$

Throughout the dynamic evolution of multipartite cavity-reservoir systems, the quantum state of subsystem c_1r_2 is $\rho_{c_1r_2}(t) = \mathrm{tr}_{r_1c_2}[\rho_{c_1r_1c_2r_2}(t)]$, which can be written as

$$\rho_{c_1r_2}(t) = \begin{pmatrix}
b_{11} & 0 & 0 & 0 & 0 & b_{16} & 0 & 0\\
0 & b_{22} & 0 & 0 & 0 & 0 & b_{27} & 0\\
0 & 0 & b_{33} & 0 & 0 & 0 & 0 & b_{38}\\
0 & 0 & 0 & b_{44} & 0 & 0 & 0 & 0\\
0 & 0 & 0 & 0 & b_{55} & 0 & 0 & 0\\
b_{61} & 0 & 0 & 0 & 0 & b_{66} & 0 & 0\\
0 & b_{72} & 0 & 0 & 0 & 0 & b_{77} & 0\\
0 & 0 & b_{83} & 0 & 0 & 0 & 0 & b_{88}
\end{pmatrix}, \tag{C1}$$

where the nonzero matrix elements are

$$\begin{aligned}
b_{11} &= [p+(1-p)\xi^4](1+\xi^2\chi^2)/2,\\
b_{22} &= \{2(1-p)\xi^2\chi^2+[p+3(1-p)\xi^4]\chi^4\}/2,\\
b_{33} &= (1-p)\chi^4(1+3\xi^2\chi^2)/2,
\end{aligned}$$

$$
\begin{aligned}
b_{44} &= (1-p)\chi^8/2,\\
b_{55} &= [\xi^8 + p(\xi^4-\xi^8)]/2,\\
b_{66} &= \xi^2\chi^2[p+3(1-p)\xi^4]/2,\\
b_{77} &= 3(1-p)\xi^4\chi^4/2,\\
b_{88} &= (1-p)\xi^2\chi^6/2,\\
b_{16} &= b_{61} = \xi\chi[p+\sqrt{3}(1-p)\xi^4]/2,\\
b_{27} &= b_{72} = \sqrt{3/2}(1-p)\xi^3\chi^3,\\
b_{38} &= b_{83} = (1-p)\xi\chi^5/2.
\end{aligned}
\tag{C2}
$$

For this quantum state, the negativity is

$$
N_{c_1r_2}(t) = \frac{\sum_{i=1}^{8}|\lambda_i|-1}{2}, \tag{C3}
$$

where λ_i are the eigenvalues of the partial transpose matrix $\rho_{c_1r_2}^{T_{c_1}}$ and have the form

$$
\begin{aligned}
\lambda_1 &= (1-p)\xi^2\chi^6/2,\\
\lambda_2 &= (1+\xi^2\chi^2)[p+(1-p)\xi^4]/2,\\
\lambda_3 &= [1-2\chi^2+B_1-\sqrt{1-(1-p)\chi^2B_2}]/4,\\
\lambda_4 &= [1-2\chi^2+B_1+\sqrt{1-(1-p)\chi^2B_2}]/4,\\
\lambda_5 &= [(3-2p)\chi^2+B_3-\sqrt{\chi^4B_4}]/4,\\
\lambda_6 &= [(3-2p)\chi^2+B_3+\sqrt{\chi^4B_4}]/4,\\
\lambda_7 &= [(1-p)\chi^4(3\xi^4+\chi^4)-\sqrt{(1-p)^2B_5}]/4,\\
\lambda_8 &= [(1-p)\chi^4(3\xi^4+\chi^4)+\sqrt{(1-p)^2B_5}]/4,
\end{aligned}
\tag{C4}
$$

with the parameters

$$
\begin{aligned}
B_1 &= (7-5p)\chi^4 - 10(1-p)\chi^6 + (4-4p)\chi^8,\\
B_2 &= (16-8\sqrt{3})p + [14-24(2-\sqrt{3})p]\chi^2\\
&\quad -8[8-(10-3\sqrt{3})p]\chi^4 + [123-(111-8\sqrt{3})p]\chi^6\\
&\quad -(104-96p)\chi^8 + 28(1-p)\chi^{10} + (8-8p)\chi^{12}\\
&\quad -4(1-p)\chi^{14},\\
B_3 &= -(8-7p)\chi^4 + 12(1-p)\chi^6 - 6(1-p)\chi^8,\\
B_4 &= (3-2p)^2 - [36-2(23-6p)p]\chi^2\\
&\quad +(64-96p+33p^2)\chi^4 - 12(1-p)(4-3p)\chi^6\\
&\quad -12(1-p)^2\chi^8,\\
B_5 &= \chi^8(9\xi^8+4\xi^2\chi^2-6\xi^4\chi^4+\chi^8).
\end{aligned}
\tag{C5}
$$

APPENDIX D: THE ESD FOR THE MMESS WITH HIGHER-DIMENSIONAL COMPONENTS

In the multipartite cavity-reservoir systems, we first consider that the two cavities are initially in the MMES,

$$
\rho_{c_1c_2}^{(1)}(0) = p|\psi_1\rangle\langle\psi_1| + (1-p)|\psi_3\rangle\langle\psi_3|, \tag{D1}
$$

where $|\psi_1\rangle = (|00\rangle+|11\rangle)/\sqrt{2}$ is the two-qubit Bell state and $|\psi_3\rangle = (|04\rangle+|15\rangle)/\sqrt{2}$ is the high-dimensional component. Along with the evolution of cavity-reservoir systems, the output state is

$$
\begin{aligned}
\rho_{c_1r_1c_2r_2}^{(1)}(t) = \frac{p}{2}&\big[\big(|\phi_0\rangle_{c_1r_1}|\phi_0\rangle_{c_2r_2} + |\phi_1^t\rangle_{c_1r_1}|\phi_1^t\rangle_{c_2r_2}\big)\\
&\times\big(\langle\phi_0|_{c_1r_1}\langle\phi_0|_{c_2r_2} + \langle\phi_1^t|_{c_1r_1}\langle\phi_1^t|_{c_2r_2}\big)\big]\\
&+\frac{1-p}{2}\big[\big(|\phi_0\rangle_{c_1r_1}|\phi_4^t\rangle_{c_2r_2} + |\phi_1^t\rangle_{c_1r_1}|\phi_5^t\rangle_{c_2r_2}\big)\\
&\times\big(\langle\phi_0|_{c_1r_1}\langle\phi_4^t|_{c_2r_2} + \langle\phi_1^t|_{c_1r_1}\langle\phi_5^t|_{c_2r_2}\big)\big],
\end{aligned}
\tag{D2}
$$

where the components have the forms

$$
\begin{aligned}
|\phi_0^t\rangle &= |00\rangle,\\
|\phi_1^t\rangle &= \xi|10\rangle + \chi|01\rangle,\\
|\phi_4^t\rangle &= \xi^4|40\rangle + 2\xi^3\chi|31\rangle + \sqrt{6}\xi^2\chi^2|22\rangle\\
&\quad + 2\xi\chi^3|13\rangle + \chi^4|04\rangle,\\
|\phi_5^t\rangle &= \xi^5|50\rangle + \sqrt{5}\xi^4\chi|41\rangle + \sqrt{10}\xi^3\chi^2|32\rangle\\
&\quad + \sqrt{10}\xi^2\chi^3|23\rangle + \sqrt{5}\xi\chi^4|14\rangle + \chi^5|05\rangle,
\end{aligned}
\tag{D3}
$$

with the parameters $\xi(t) = e^{-\kappa t/2}$ and $\chi(t) = (1-e^{-\kappa t})^{1/2}$. By tracing the subsystems of two reservoirs, we can get the output state of two cavities $\rho_{c_1c_2}^{(1)}(t) = \mathrm{Tr}_{r_1r_2}[\rho_{c_1r_1c_2r_2}^{(1)}(t)]$, which is a 12×12 matrix. In order to obtain the entanglement negativity of $\rho_{c_1c_2}^{(1)}(t)$, we calculate the eigenvalues of the partial transpose matrix $\rho_{c_1c_2}^{(1)T_{c_1}}(t)$. After some derivation, we find that there are four eigenvalues which can be negative,

$$
\begin{aligned}
\lambda_2 &= (1-p)\xi^{10}(3\chi^2-\sqrt{1+4\chi^4})/2,\\
\lambda_6 &= (1-p)\xi^8(1+15\chi^4-\sqrt{1+70\chi^4+25\chi^8})/4,\\
\lambda_7 &= (1-p)\xi^6\chi^2(1+5\chi^4-\sqrt{1+15\chi^4}),\\
\lambda_{11} &= \xi^2\chi^2[\chi^4(2+3\chi^4)+p(1-2\chi^4-3\chi^8)]/2 - \sqrt{H_1}/2,
\end{aligned}
\tag{D4}
$$

where the parameter is $H_1 = \xi^4[p^2+2\sqrt{5}(1-p)p\chi^8 + (1-p)^2(4\chi^{12}+13\chi^{16}+4\chi^{20})]$. Similar to the analysis in Appendix A, we can derive the ESD time for the MMES $\rho_{c_1c_2}^{(1)}(t)$ according to the four eigenvalues. When the mixed-state probability p changes in the region $[0,p_1]$ with $p_1 = (347-125\sqrt{5})/1922 \approx 0.03512$, the ESD time for the MMES is $\kappa t = \ln[(5+\sqrt{5})/4] \approx 0.5928$. When the probability $p\in[p_1,1)$, the ESD time is determined by the $p\sim\kappa t$ relation

$$
p = \frac{\sqrt{2}\chi^8\sqrt{J_1}+\chi^8J_2}{1-\chi^4+2(2-\sqrt{5})\chi^8+6\chi^{12}+\chi^{16}-5\chi^{20}}, \tag{D5}
$$

where the two parameters are $J_1 = 4-2\sqrt{5}+3(3-\sqrt{5})\chi^4+2\chi^8$ and $J_2 = 2-\sqrt{5}+3\chi^4+\chi^8-5\chi^{12}$. In Fig. 6(a), we plot the ESD line (red line) as a function $p(\kappa t)$, which divides the entanglement evolution into an entangled region and a disentangled region.

Next, we consider the two cavities which are initially in the MMES,

$$
\rho_{c_1c_2}^{(2)}(0) = p|\psi_1\rangle\langle\psi_1| + (1-p)|\psi_4\rangle\langle\psi_4|, \tag{D6}
$$

where $|\psi_4\rangle = (|06\rangle+|17\rangle)/\sqrt{2}$ is the high-dimensional component. As the systems evolves, the output state $\rho_{c_1r_1c_2r_2}^{(2)}(t)$ has

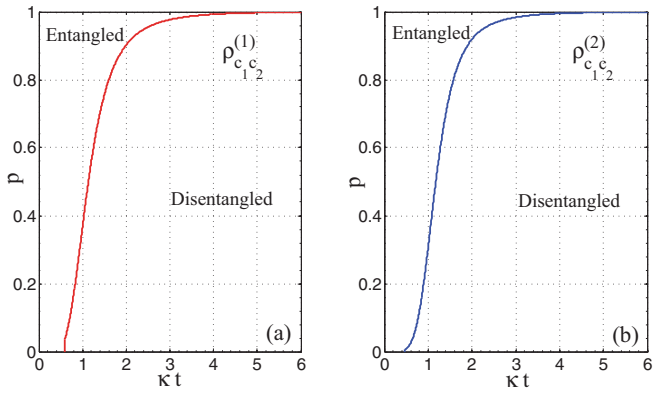

FIG. 6. The ESD lines in the evolution of two cavities which are initially in the MMESs: (a) $\rho^{(1)}_{c_1c_2}$ in Eq. (D1) and (b) $\rho^{(2)}_{c_1c_2}$ in Eq. (D6).

the same form as that in Eq. (D2), but the components $|\phi^t_4\rangle$ and $|\phi^t_5\rangle$ are replaced by the new components $|\phi^t_6\rangle$ and $|\phi^t_7\rangle$, which can be written as

$$\begin{aligned}|\phi^t_6\rangle &= \xi^6|60\rangle + \sqrt{6}\xi^5\chi|51\rangle + \sqrt{15}\xi^4\chi^2|42\rangle \\ &\quad + \sqrt{20}\xi^3\chi^3 + \sqrt{15}\xi^2\chi^4 + \sqrt{6}\xi\chi^5|15\rangle + \chi^6|06\rangle, \\ |\phi^t_7\rangle &= \xi^7|70\rangle + \sqrt{7}\xi^6\chi|61\rangle + \sqrt{21}\xi^5\chi^2|52\rangle \\ &\quad + \sqrt{35}\xi^4\chi^3|43\rangle + \sqrt{35}\xi^3\chi^4|34\rangle + \sqrt{21}\xi^2\chi^5|25\rangle \\ &\quad + \sqrt{7}\xi\chi^6|16\rangle + \chi^7|07\rangle. \end{aligned} \tag{D7}$$

After tracing the subsystems r_1r_2, we can get the output state of two cavities $\rho^{(2)}_{c_1c_2}(t)$. Furthermore, by doing the partial transposition, we can obtain the matrix $\rho^{(2)T_{c_1}}_{c_1c_2}(t)$ and calculate its eigenvalues. The ESD line is determined by the negative eigenvalues of $\rho^{(2)T_{c_1}}_{c_1c_2}(t)$. When the mixed-state probability $p \in [0, p_2]$, with $p_2 = (8669 - 2401\sqrt{7})/370191 \approx 0.006258$, the ESD occurs at the time $\kappa t = \ln[(7+\sqrt{7})/6] \approx 0.4748$. When $p \in [p_2, 1)$, the ESD time is determined by the following $p \sim \kappa t$ relation:

$$p = \frac{\chi^{12}(K_1 + \sqrt{K_2})}{1 - \chi^4 + 2(3-\sqrt{7})\chi^{12} + 8\chi^{16} + \chi^{24} - 7\chi^{28}}, \tag{D8}$$

where the two parameters are $K_1 = 3 - \sqrt{7} + 4\chi^4 + \chi^{12} - 7\chi^{16}$ and $K_2 = 15 - 6\sqrt{7} + 8(4-\sqrt{7})\chi^4 + 9\chi^8$. In Fig. 6(b), we plot the ESD line (blue line) as a function $p(\kappa t)$, which cut the entanglement evolution region into two parts, i.e., an entangled region and a disentangled region.

APPENDIX E: THE MIN OF THE MMES WITH HIGHER-DIMENSIONAL COMPONENTS AND ITS DISTRIBUTION

We first consider the MMES $\rho^{(1)}_{c_1c_2}(0)$ with the high-dimensional component $|\psi_3\rangle = (|04\rangle + |15\rangle)/\sqrt{2}$, as shown in Eq. (D1). According to the formula in Eq. (18) of the main text, we can derive the nonlocality

$$\mathrm{MIN}\big[\rho^{(1)}_{c_1c_2}(0)\big] = (p - 1/2)^2 + 1/4, \tag{E1}$$

which is dependent on the mixed-state probability p and directly proportional to the purity of the MMES. In the calculation of the MIN, the matrix basis for the subsystem c_2 is chosen to be the generalized Gell-Mann matrices (GGM) [61], which are the higher-dimensional extension of the Pauli matrices. The GGM basis for a d-dimensional system is composed of three types of matrices [61]: (i) $d(d-1)/2$ symmetric GGM,

$$\Lambda^{jk}_s = |j\rangle\langle k| + |k\rangle\langle j|, \quad 1 \leqslant j < k \leqslant d; \tag{E2}$$

(ii) $d(d-1)/2$ antisymmetric GGM,

$$\Lambda^{jk}_a = -i|j\rangle\langle k| + i|k\rangle\langle j|, \quad 1 \leqslant j < k \leqslant d; \tag{E3}$$

and (iii) $(d-1)$ diagonal GGM,

$$\Lambda^l = \sqrt{2/(l^2+l)}\left(\sum_{j=1}^{l}|j\rangle\langle j| - l|l+1\rangle\langle l+1|\right), \tag{E4}$$

with $1 \leqslant l \leqslant d-1$. It should be noted that the GGM needs to be normalized in the generalized Bloch form of $\rho^{(1)}_{c_1c_2}$. Along with the interaction between the cavities and reservoirs, the MMES will evolve into a $2 \otimes 6$ system. After some derivation, we obtain

$$\mathrm{MIN}\big[\rho^{(1)}_{c_1c_2}(t)\big] = \frac{\xi^4}{2}\{\xi^{16} + p[p - (2-p)\xi^{16}] + L_1 + L_2\}, \tag{E5}$$

where the two parameters are $L_1 = 2(1-p)[\sqrt{5}p + 30(1-p)\xi^8]\chi^8$ and $L_2 = (1-p)^2(20\xi^{12}\chi^4 + 40\xi^4\chi^{12} + 5\chi^{16})$. In the dissipative procedure of cavity-reservoir systems, the nonlocality of two cavities decays in an asymptotical way, which is similar to the case of MMES in $2 \otimes 4$ systems.

Next, we analyze the MMES of a $2 \otimes 8$ system in Eq. (D6), which has the high-dimensional component $|\psi_4\rangle = (|06\rangle + |17\rangle)/\sqrt{2}$. It is found that the MIN for this MMES $\rho^{(2)}_{c_1c_2}(0)$ has the same expression as that in Eq. (E1), which is also dependent on the mixed-state probability p. As the system evolves, the MIN for two cavities decays asymptotically and can be expressed as

$$\mathrm{MIN}\big[\rho^{(2)}_{c_1c_2}(t)\big] = \frac{\xi^4}{2}[\xi^{24} + L_3 + (1-p)^2 L_4], \tag{E6}$$

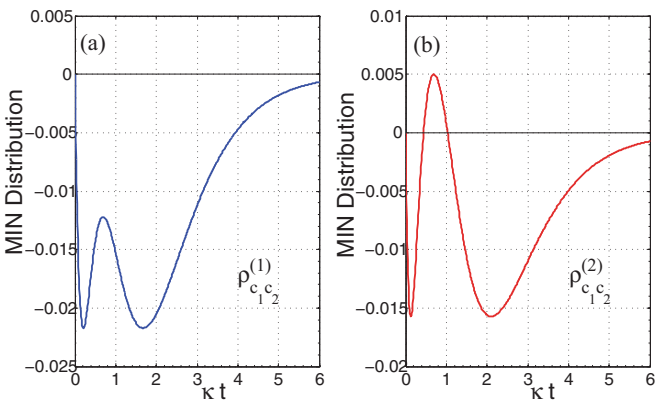

FIG. 7. The MIN distributions of the MMESs in multipartite $2 \otimes 2 \otimes 6 \otimes 6$ and $2 \otimes 2 \otimes 8 \otimes 8$ cavity-reservoir systems are plotted as a function of κt, where the negative values indicate that the MIN is not monogamous.

where the parameters are $L_3 = p[p-(2-p)\xi^{24}] + 2(1-p)[\sqrt{7}p + 350(1-p)\xi^{12}]\chi^{12}$ and $L_4 = 42\xi^{20}\chi^4 + 315\xi^{16}\chi^8 + 525\xi^8\chi^{16} + 126\xi^4\chi^{20} + 7\chi^{24}$.

For the MMESs $\rho^{(1)}_{c_1c_2}(0)$ and $\rho^{(2)}_{c_1c_2}(0)$ with the high-dimensional components, we further calculate the distribution

$$M'_{c_1r_1|c_2r_2}(t) = \mathrm{MIN}_{c_1r_1|c_2r_2}(t) - \mathrm{MIN}_{c_1c_2}(t) - \mathrm{MIN}_{c_1r_2}(t) - \mathrm{MIN}_{r_1c_2}(t) - \mathrm{MIN}_{r_1r_2}(t) \quad \text{(E7)}$$

in the multipartite cavity-reservoir systems. We find that the MIN distributions are still not monogamous. As examples, we choose the mixed-state probability $p = 0.8$ for the two MMESs and calculate their MIN distributions. In Fig. 7, the MIN distributions in the multipartite systems are plotted, where two cavities are initially in the MMESs $\rho^{(1)}_{c_1c_2}(0)$ and $\rho^{(2)}_{c_1c_2}(0)$. As shown, the negative values for the distributions indicate that the MIN is not monogamous.

However, for the squared negativity of the MMESs in $2 \otimes 6$ and $2 \otimes 8$ systems, we calculate the entanglement distribution in the multipartite $2 \otimes 2 \otimes 6 \otimes 6$ and $2 \otimes 2 \otimes 8 \otimes 8$ cavity-reservoir systems, where the mixed-state probability p ranges across $[0,1]$. The numerical results still support that the negativity is monogamous.

[1] R. Horodecki, P. Horodecki, M. Horodecki, and K. Horodecki, Rev. Mod. Phys. **81**, 865 (2009).
[2] C. Eltschka and J. Siewert, J. Phys. A **47**, 424005 (2014).
[3] J. Cui, M. Gu, L. C. Kwek, M. F. Santos, H. Fan, and V. Vedral, Nat. Commun. **3**, 812 (2012).
[4] C. H. Bennett, G. Brassard, C. Crépeau, R. Jozsa, A. Peres, and W. K. Wootters, Phys. Rev. Lett. **70**, 1895 (1993).
[5] A. K. Ekert, Phys. Rev. Lett. **67**, 661 (1991).
[6] C. H. Bennett and S. J. Wiesner, Phys. Rev. Lett. **69**, 2881 (1992).
[7] D. Cavalcanti, F. G. S. L. Brandão, and M. O. Terra Cunha, Phys. Rev. A **72**, 040303 (2005).
[8] Z. G. Li, M. J. Zhao, S. M. Fei, H. Fan, and W. M. Liu, Quantum Inf. Comput. **12**, 0063 (2012).
[9] M.-J. Zhao, Phys. Rev. A **91**, 012310 (2015).
[10] K. Życzkowski, P. Horodecki, M. Horodecki, and R. Horodecki, Phys. Rev. A **65**, 012101 (2001).
[11] S. Scheel, J. Eisert, P. L. Knight, and M. B. Plenio, J. Mod. Opt. **50**, 881 (2003).
[12] T. Yu and J. H. Eberly, Phys. Rev. Lett. **93**, 140404 (2004).
[13] M. P. Almeida, F. de Melo, M. Hor-Meyll, A. Salles, S. P. Walborn, P. H. Souto Ribeiro, and L. Davidovich, Science **316**, 579 (2007).
[14] J. Laurat, K. S. Choi, H. Deng, C. W. Chou, and H. J. Kimble, Phys. Rev. Lett. **99**, 180504 (2007).
[15] T. Yu and J. H. Eberly, Science **323**, 598 (2009).
[16] C. E. López, G. Romero, F. Lastra, E. Solano, and J. C. Retamal, Phys. Rev. Lett. **101**, 080503 (2008).
[17] C. H. Bennett, D. P. DiVincenzo, C. A. Fuchs, T. Mor, E. Rains, P. W. Shor, J. A. Smolin, and W. K. Wootters, Phys. Rev. A **59**, 1070 (1999).
[18] H. Buhrman, R. Cleve, S. Massar, and R. de Wolf, Rev. Mod. Phys. **82**, 665 (2010).
[19] S. Luo and S. Fu, Phys. Rev. Lett. **106**, 120401 (2011).
[20] J. S. Bell, Physics **1**, 195 (1964).
[21] J. F. Clauser, M. A. Horne, A. Shimony, and R. A. Holt, Phys. Rev. Lett. **23**, 880 (1969).
[22] G. Vidal and R. F. Werner, Phys. Rev. A **65**, 032314 (2002).
[23] Y.-K. Bai, M.-Y. Ye, and Z. D. Wang, Phys. Rev. A **80**, 044301 (2009).
[24] W. Wen, Y.-K. Bai, and H. Fan, Eur. Phys. J. D **64**, 557 (2011).
[25] M. Ali and A. R. P. Rau, Phys. Rev. A **90**, 042330 (2014).
[26] In order to conveniently obtain the output state in Eq. (8), we can introduce an environment system E which purifies the quantum state $\rho_{c_1c_2}$. Then the global initial state can be written as $|\Psi(0)\rangle = (\sqrt{p}|\psi_1\rangle_{c_1c_2}|0\rangle_E + \sqrt{1-q}|\psi_2\rangle_{c_1c_2}|1\rangle_E)|00\rangle_{r_1r_2}$, and the global output state $|\Psi(t)\rangle$ can be obtained via the components in Eq. (9). After tracing the environment system E, we can get the output state.
[27] C. H. Bennett, H. J. Bernstein, S. Popescu, and B. Schumacher, Phys. Rev. A **53**, 2046 (1996).
[28] V. Coffman, J. Kundu, and W. K. Wootters, Phys. Rev. A **61**, 052306 (2000).
[29] T. J. Osborne and F. Verstraete, Phys. Rev. Lett. **96**, 220503 (2006).
[30] Y.-K. Bai, D. Yang, and Z. D. Wang, Phys. Rev. A **76**, 022336 (2007).
[31] Y.-K. Bai, Y.-F. Xu, and Z. D. Wang, Phys. Rev. Lett. **113**, 100503 (2014).
[32] C. Eltschka and J. Siewert, Phys. Rev. Lett. **114**, 140402 (2015).
[33] Y.-C. Ou and H. Fan, Phys. Rev. A **75**, 062308 (2007).
[34] H. He and G. Vidal, Phys. Rev. A **91**, 012339 (2015).
[35] R. Lohmayer, A. Osterloh, J. Siewert, and A. Uhlmann, Phys. Rev. Lett. **97**, 260502 (2006).
[36] Y.-K. Bai and Z. D. Wang, Phys. Rev. A **77**, 032313 (2008).
[37] Y.-K. Bai, M.-Y. Ye, and Z. D. Wang, Phys. Rev. A **78**, 062325 (2008).
[38] B. Regula, S. Di Martino, S. Lee, and G. Adesso, Phys. Rev. Lett. **113**, 110501 (2014)
[39] G. H. Aguilar, A. Valdés-Hernández, L. Davidovich, S. P. Walborn, and P. H. Souto Ribeiro, Phys. Rev. Lett. **113**, 240501 (2014).
[40] A. Sen, D. Sarkar, and A. Bhar, J. Phys. A **45**, 405306 (2012).
[41] Q. Lin, Y.-K. Bai, M.-Y. Ye, and X.-M. Lin, Chin. Phys. B **24**, 030304 (2015).
[42] H. Ollivier and W. H. Zurek, Phys. Rev. Lett. **88**, 017901 (2001).
[43] L. Henderson and V. Vedral, J. Phys. A **34**, 6899 (2001).
[44] R. Prabhu, A. K. Pati, A. Sen(De), and U. Sen, Phys. Rev. A **85**, 040102 (2012).
[45] A. Streltsov, G. Adesso, M. Piani, and D. Bruß, Phys. Rev. Lett. **109**, 050503 (2012).
[46] G. L. Giorgi, Phys. Rev. A **84**, 054301 (2011).
[47] F. F. Fanchini, M. C. de Oliveira, L. K. Castelano, and M. F. Cornelio, Phys. Rev. A **87**, 032317 (2013).
[48] Y.-K. Bai, N. Zhang, M.-Y. Ye, and Z. D. Wang, Phys. Rev. A **88**, 012123 (2013).
[49] K. Salini, R. Prabhu, A. Sen(De), and U. Sen, Ann. Phys. (NY) **348**, 297 (2014).

[50] T. R. de Oliveira, M. F. Cornelio, and F. F. Fanchini, Phys. Rev. A **89**, 034303 (2014).
[51] X.-N. Zhu and S.-M. Fei, Phys. Rev. A **90**, 024304 (2014).
[52] Y.-K. Bai, Y.-F. Xu, and Z. D. Wang, Phys. Rev. A **90**, 062343 (2014).
[53] Y. Luo and Y. Li, Ann. Phys. (NY) **362**, 511 (2015).
[54] W. Song, Y.-K. Bai, M. Yang, M. Yang, and Z.-L. Cao, Phys. Rev. A **93**, 022306 (2016).
[55] S. Ghose, N. Sinclair, S. Debnath, P. Rungta, and R. Stock, Phys. Rev. Lett. **102**, 250404 (2009).
[56] R. Augusiak, D. Cavalcanti, G. Prettico, and A. Acín, Phys. Rev. Lett. **104**, 230401 (2010).
[57] R. Gallego, L. E. Würflinger, A. Acín, and M. Navascués, Phys. Rev. Lett. **109**, 070401 (2012).
[58] T. Vértesi and N. Brunner, Phys. Rev. Lett. **108**, 030403 (2012).
[59] F. Buscemi, Phys. Rev. Lett. **108**, 200401 (2012).
[60] Y.-C. Liang, F. J. Curchod, J. Bowles, and N. Gisin, Phys. Rev. Lett. **113**, 130401 (2014).
[61] R. A. Bertlmann and P. Krammer, J. Phys. A **41**, 235303 (2008).